International Journal of Concrete Structures and Materials

RESEARCH Open Access

Experimental Evaluation of Tension and Shear Capacities of New Headed Cast-in Specialty Inserts in Cracked Concrete

Sang-Deock Jeong[1], Chang-Soo Oh[2] and Chang-Hwan Lee[3*]

Abstract

Headed cast-in specialty inserts are often developed and employed for their improved constructability and time-saving benefits over traditional cast-in and post-installed anchors. Their acceptance criteria (AC 446) were established by The International Code Council Evaluation Service. However, previous research on the behavioral characteristics of headed specialty inserts is rare. This study investigates the performance of a newly developed insert anchor for use as an earthquake-resistant anchor for fire protection systems and suspended lightweight piping. Firstly, three cyclic tension tests of the specialty insert with a threaded rod were conducted in accordance with AC 446. These tests resulted in all experimental subjects achieving the target strength without defects. Subsequently, monotonic tension and shear tests of the insert anchor in cracked concrete were performed five times each to assess the tensile and shear capacities of the new insert anchor. The results were compared with the nominal strength determined by the anchor design equation provided by the ACI 318 for cast-in headed anchors, finding that the latter adequately approximates the concrete breakout strength of the new insert anchor in tension but underestimates the concrete pryout strength in shear. Based on the measured breakout failure surface angles, a projected area of the failure cone of the corresponding anchor with a relatively large head size is proposed.

Keywords Headed cast-in specialty insert, Cracked concrete, Insert anchor, Tension strength, Shear strength, Concrete breakout, Concrete pryout, Head size

1 Introduction

In recent earthquakes, losses attributed to nonstructural damage have exceeded those related to structural losses. As a result, there has been a growing interest in the seismic design of nonstructural components in the field of earthquake engineering (Filiatrault et al., 2021; Kazantzi et al., 2020; Merino et al., 2020). In addition, increasing attention has been given to the design and construction of the anchors that constitute the fixed part of nonstructural components (Kim et al., 2022; Mahrenholtz & Wood, 2021). Numerous cast-in anchors (Delhomme et al., 2015; Jang & Suh, 2006; Petersen et al., 2021) and post-installed anchors (Hoehler et al., 2011; Kim et al., 2004; Mahrenholtz et al., 2010) have been developed and studied, as traditional methods of fixing nonstructural components to structural concrete. Moreover, headed cast-in specialty inserts have been developed and are commonly used to improve constructability and reduce construction time of cast-in and post-installed anchors (Zamani, 2019). The International Code Council Evaluation Service has established acceptance criteria for these

Journal information: ISSN 1976-0485 / eISSN 2234-1315

*Correspondence:
Chang-Hwan Lee
chlee@pknu.ac.kr
[1] Division of Architectural and Fire Protection Engineering, Pukyong National University, 45, Yongso-ro, Nam-gu, Busan 48513, Republic of Korea
[2] Yangsoo Metals Co., Ltd., 76-6, Cheoyong Industrial 1-gil, Onsan-eup, Ulju-gun, Ulsan 44993, Republic of Korea
[3] Department of Architectural Engineering, Pukyong National University, 45, Yongso-ro, Nam-gu, Busan 48513, Republic of Korea

inserts (ICC-ES, 2018). However, studies on the detailed behavioral characteristics and performance analysis of these specialty inserts have been limited.

To address this issue, a new type of headed cast-in specialty insert was developed for use as an earthquake-resistant anchor for suspended lightweight piping and fire protection systems. Jeon et al. (2021) conducted tests to evaluate the monotonic tension and shear capacities of corresponding inserts in uncracked concrete, using a threaded rod with a nominal tensile strength (F_{tn}) of 400 MPa. Of the six tensile strength specimens tested, three failed due to concrete breakout. Additionally, the projected area of the failure surface was significantly larger than the projected concrete failure area (A_{Nc}) specified by the ACI 318 (ACI, 2019). This discrepancy may be attributed to the diameter of the anchor head (d_h) in headed specialty inserts, which is larger than that of general cast-in headed anchors. Therefore, further research and detailed analysis are required to prevent underestimation of the anchor group effects associated with headed specialty inserts.

ACI 318 currently determines A_{Nc} by using the idealized pyramid model of the concrete capacity design (CCD) method, which assumes a breakout failure surface angle (α) of 35° (Fuchs et al., 1995). Thus, the critical edge distance (c_{cr}) is set to 1.5 times the effective embedment depth of the anchor (h_{ef}), and A_{Nc} is determined for a single anchor as $9h_{ef}^2$ ($=3h_{ef}\times 3h_{ef}$). However, several previous studies on large-headed anchors have suggested that the head size of the anchor should also be considered in the design (Di Nunzio & Muciaccia, 2000; Karmokar et al., 2021; Lee et al., 2007; Nilforoush et al., 2017, 2018; Ožbolt et al., 2007). Karmokar et al. (2021) reviewed previous studies and reported that the range of α was between 10 and 35°, depending on h_{ef}, the head size of the anchor, and the type of concrete substrate. Lee et al. (2007) conducted monotonic tensile experiments, obtained the α of the anchor with relatively large h_{ef} and d_h of approximately 20–30°, and proposed the characteristic anchor spacing (S_{cr}) for determining the A_{Nc} of corresponding anchors as $4h_{ef}$, instead of the current $3h_{ef}$ of ACI 318. In addition, Nilforoush et al. (2017, 2018) conducted experiments and numerical analyses to investigate the application of $S_{cr}=5h_{ef}$ for the design of anchors with large d_h. Headed specialty inserts typically have large d_h but shallow h_{ef}. Therefore, based on the results of the above-mentioned studies, experimental methods are preferred for evaluating α and A_{Nc} in the design of headed specialty inserts.

The capacity of the headed cast-in specialty insert considered in this study is evaluated by AC 446 (ICC-ES, 2018). The strength values of the insert are determined in accordance with AC 446 through tension and shear tests, which are then applied to the design procedure of ACI 318. A tension test is conducted on the insert without concrete contact, while a shear test is performed on anchors in cracked concrete, following the method outlined in ACI 355.2 (ACI Committee355, 2019), which is commonly used to verify concrete anchor performance. The use of high-strength threaded rod with a tensile strength (F_t) of 150,000 psi (1034 MPa) or higher is regulated to cause failure of the insert. While the capacity of the new insert anchor in uncracked concrete has been previously evaluated, as mentioned above (Jeon et al., 2021), cracked concrete conditions can negatively affect the performance of the anchor (Lee & Jung, 2021; Vita & Sharma, 2021). In addition, even though the tension test in plain concrete is not required for the insert in concrete in AC 446, the evaluation of tensile behavior in cracked concrete is necessary according to ACI 355.2 to fully elucidate its performance.

Based on the background outlined above, this study investigates the capacity and behavioral characteristics of a new insert anchor, which is a type of headed cast-in specialty insert. Although the ACI 318 provisions for anchoring to concrete do not include headed cast-in specialty inserts as anchor types, this study aims to experimentally evaluate the strengths of the new insert anchor according to the relevant standards (AC 446 and ACI 355.2). Firstly, the components of the insert anchor are introduced, followed by the presentation of the results of the three sets of cyclic tension tests for the specialty insert with threaded rod in compliance with AC 446. Subsequently, monotonic tension and shear tests of the insert anchor in cracked concrete were performed five times each as the main experiment to evaluate the strength of the new insert anchor. The strengths obtained through the experiments are then compared with the strengths determined according to the ACI 318 provisions for cast-in headed anchors. Additionally, based on the α values measured from the tension tests, c_{cr} and A_{Nc} of the studied anchor with large d_h values are proposed to avoid unconservative consideration of anchor group effects.

2 New Insert Anchor

2.1 Overview

Fig. 1 depicts a schematic of the new insert anchor that is the subject of this study. The anchor consists of a fixing screw, lower cover, and insert, with h_{ef} and d_h measuring 50 mm and 42 mm, respectively. The installation and construction procedure of the anchor is illustrated in Fig. 2, which shows the following steps: (a) fixing the insert to the form through the fixing screw by hammering during form installation; (b) casting concrete; (c) separating the fixing screw while removing the form, and

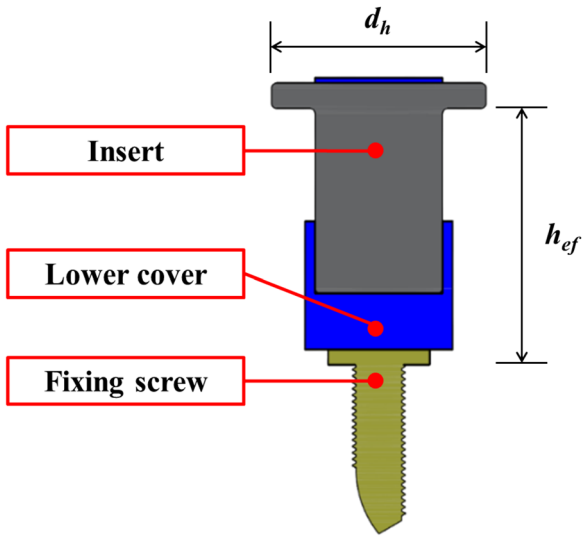

Fig. 1 Schematic of the new insert anchor under consideration

(d) introducing the threaded rod that connects the non-structural component into the insert embedded in the concrete using manual force.

The insert anchor being studied differs from other commonly used anchors, such as cast-in and post-installed anchors, by virtue of its simplified installation process, which involves pushing the threaded rod into the insert. As described previously, this simple installation process greatly reduces the workload and improves constructability. Furthermore, installing the insert prior to concrete casting prevents the generation of dust during installation, which contrasts with post-installed anchors that typically require drilling into the structure.

2.2 Cyclic Tension Test of Specialty Insert with Threaded Rod

The new insert anchor is assembled by pressurization through the use of human force, and does not require a rotation assembly. However, this type of joint between the bolt and the shaft may be prone to weakness. AC 446 mandates cyclic tension tests for specialty inserts with threaded rods that are not embedded in concrete. Additionally, the use of a high-strength threaded rod is required to prevent it from failing when assessing the capacity of the insert. The experimental results indicate that the tension strength of the threaded rod, which is intended for use with the inserts during the design stage is limited, as shown in Table 1.

As per AC 446 instructions, three cyclic tension tests were conducted for the new insert anchor. A high-strength M12 threaded rod with $F_t = 1040$ MPa was used for these tests. To comply with the requirements of AC 446, the experiments were performed with simulated seismic tension tests based on the ACI 355.2 (ACI Committee355, 2019); the corresponding load protocol

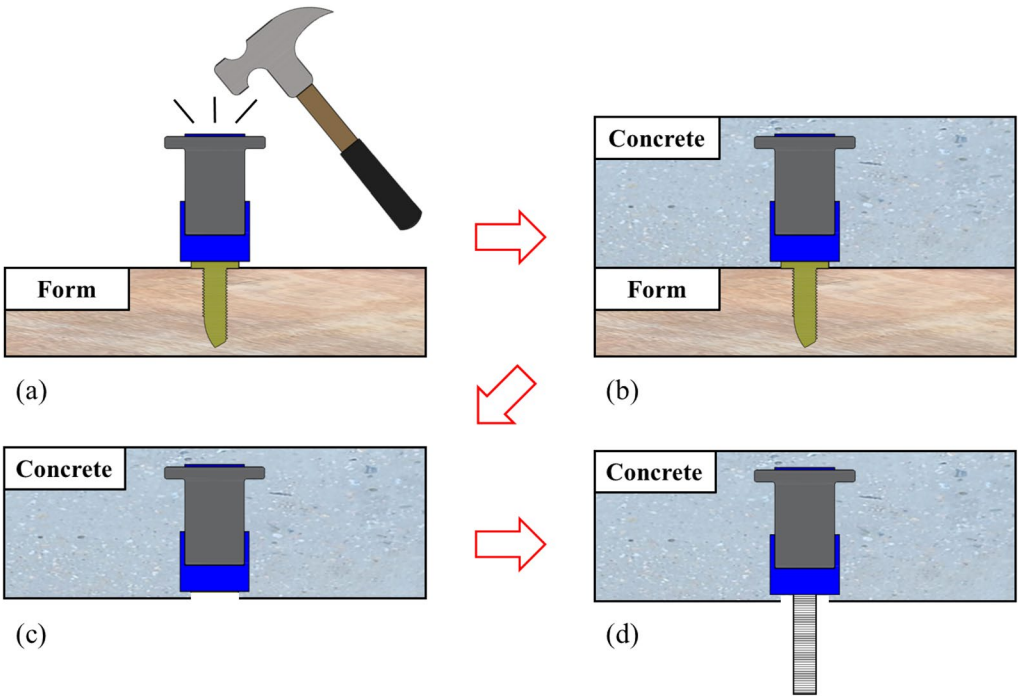

Fig. 2 Installation and construction procedure of the new insert anchor

Table 1 Tension strength requirements of the threaded rod (ICC-ES, 2018)

Group	Ratio of mean concrete breakout strength to tested strength of insert	Limit on nominal tension strength of threaded rod to be used with insert	Requirements from this experiment (kN)
A	$\frac{N_{verify}}{\overline{N}_{sa,insert,eq}} \geq 1.1$	$f_{u,bolt,max} \leq \frac{0.8\overline{N}_{sa,insert,eq}}{A_{t,bolt}}$	$\overline{N}_{sa,insert,eq} \leq 44.69$
B	$0.9 < \frac{N_{verify}}{\overline{N}_{sa,insert,eq}} < 1.1$	$f_{u,bolt,max} \leq \frac{0.8N_{verify}}{A_{t,bolt}}$	$44.69 < \overline{N}_{sa,insert,eq} < 54.62$
C	$\frac{N_{verify}}{\overline{N}_{sa,insert,eq}} \leq 0.9$	No limit	$\overline{N}_{sa,insert,eq} \geq 54.62$

N_{verify} axial tension load for which the insert shall be verified, corresponding to the mean ultimate concrete breakout strength, $\overline{N}_{sa,insert,eq}$ mean tested ultimate tension strength of specialty insert in simulated seismic tension test, $f_{u,bolt,max}$ nominal strength of threaded rod permitted to be used with specialty insert, and $A_{t,bolt}$ net tensile area of threaded rod used with specialty insert (84.3 mm^2)

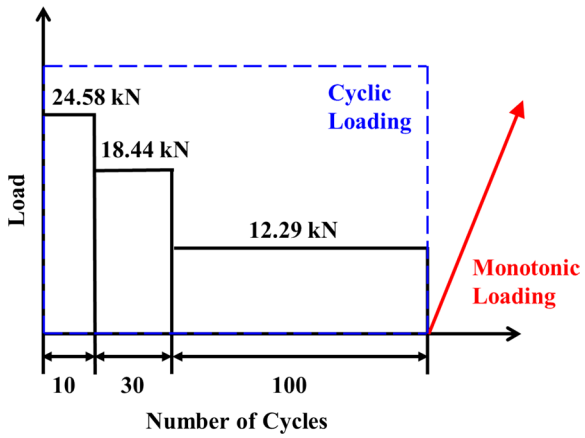

Fig. 3 Applied cyclic load protocol

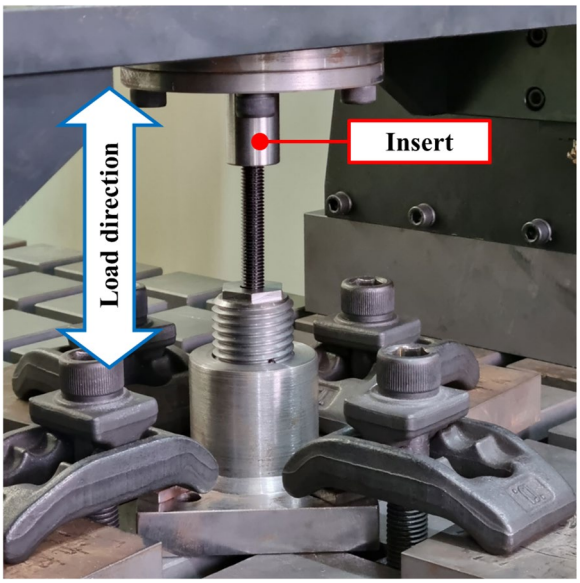

Fig. 4 Test setup for cyclic tension tests

is presented in Fig. 3. The maximum load applied (N_{eq}) was 24.58 kN, which was half of the N_{verify} determined by Eq. (1) in AC 446:

$$N_{\text{verify}} = 40\sqrt{f_c'}h_{ef}^{1.5} = 11050\text{lb} = 49.16\text{kN}, \quad (1)$$

where the specified compressive strength of concrete (f_c') is 10,000 psi (68.95 MPa), and h_{ef} is 1.969 in (50 mm). N_{eq} ($=0.5N_{verify}$) was repeated for 10 cycles, followed by an intermediate load of 18.44 kN ($=0.75N_{eq}$) and minimum load of 12.29 kN ($=0.5N_{eq}$), which were successively repeated for 30 and 100 cycles, respectively. Thereafter, the insert was subjected to monotonically increasing tensile loading to determine its residual capacity. The frequency of the cyclic loading was 1 Hz, and the loading rate of the monotonic loading was 2 mm/min. The experimental subjects were labeled as T-Insert 1 to 3, according to the order of loading. The test setup is shown in Fig. 4.

Fig. 5 displays the load–displacement curves. During cyclic loading, no damages were observed in any of the experimental subjects. In this experiment, the residual capacity was set at 60 kN during the final monotonic loading. All three subjects achieved this strength, and no visible damage was observed until the experiment's conclusion. The column on the far right of Table 1 shows the requirements of this experiment for $\overline{N}_{sa,insert,eq}$ that apply the N_{verify} determined by Eq. (2). Considering the load

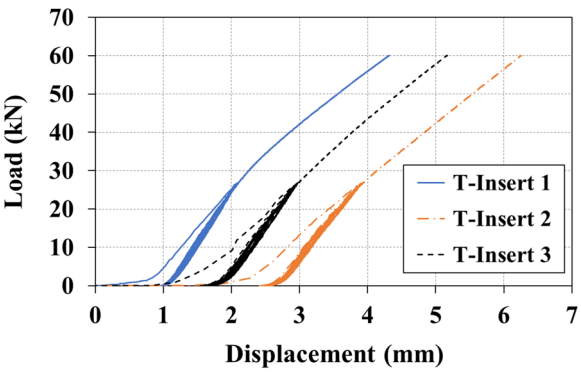

Fig. 5 Load–displacement curves of specialty insert specimens

value tested limit of 60 kN as $\overline{N}_{sa,insert,eq}$, this insert corresponds to Group C of Table 1. Thus, the threaded rod to be used with the specialty insert is not restricted by the least upper bound of F_m. Therefore, the tension strength of the insert itself, including the bolt to shaft connection, was deemed sufficient.

3 Monotonic Tension and Shear Tests in Cracked Concrete

3.1 Test Method

To evaluate the capacity of the new insert anchor in concrete, monotonic tension and shear tests were performed on cracked concrete specimens. The concrete block had dimensions of 540 mm (width) × 540 mm (length) × 200 mm (height), as shown in Fig. 6. An initial crack with a 0.5 mm width was created in accordance with the relevant standard (ACI Committee 355, 2019; ICC-ES, 2018). The manufacturing process of the cracked concrete block is described in detail in Sect. 3.2. Ten specimens were tested for both tensile and shear performance using an M12 threaded rod with an F_t of 1040 MPa, as used in the cyclic tension test of the insert described above. A displacement-controlled load was applied using a 250 kN-capacity universal testing machine (UTM), with a loading rate of 2 mm/min until a displacement of 12 mm was reached, and of 3 mm/min thereafter.

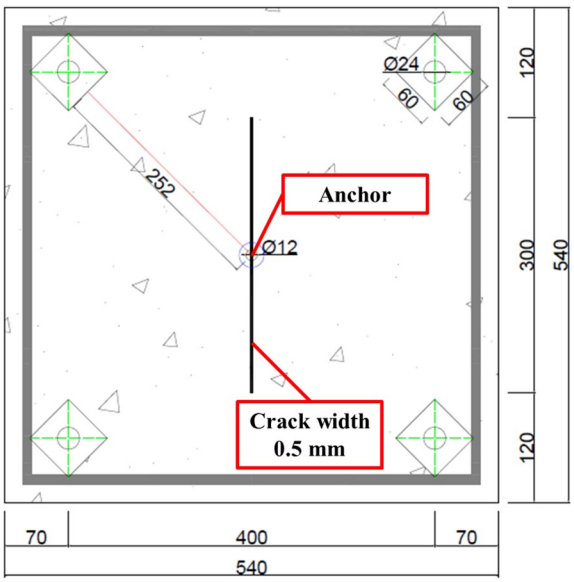

Fig. 6 Cracked concrete specimens (unit: mm)

Fig. 7 shows the test setup used. In the tension tests, the load and displacement data of the anchor were collected through the loading device. The crack width was measured using pi-type linear variable differential transducers (LVDTs) installed on both sides of the anchor, with a separation of 50 mm from the anchor center, as shown in Fig. 7a. The tension specimens were labeled as T-M-1 to T-M-5 according to the order of loading. In the shear tests, the load was applied parallel to the crack direction. The anchor displacement was measured directly by connecting the wire LVDT to the threaded rod, and the load value was obtained through the loading device. To monitor the change in crack width during the shear tests, only one side was measured, as the load jig caused an interruption, and the measurement points were located 75 mm and 150 mm away from the anchor, as shown in Fig. 7b.

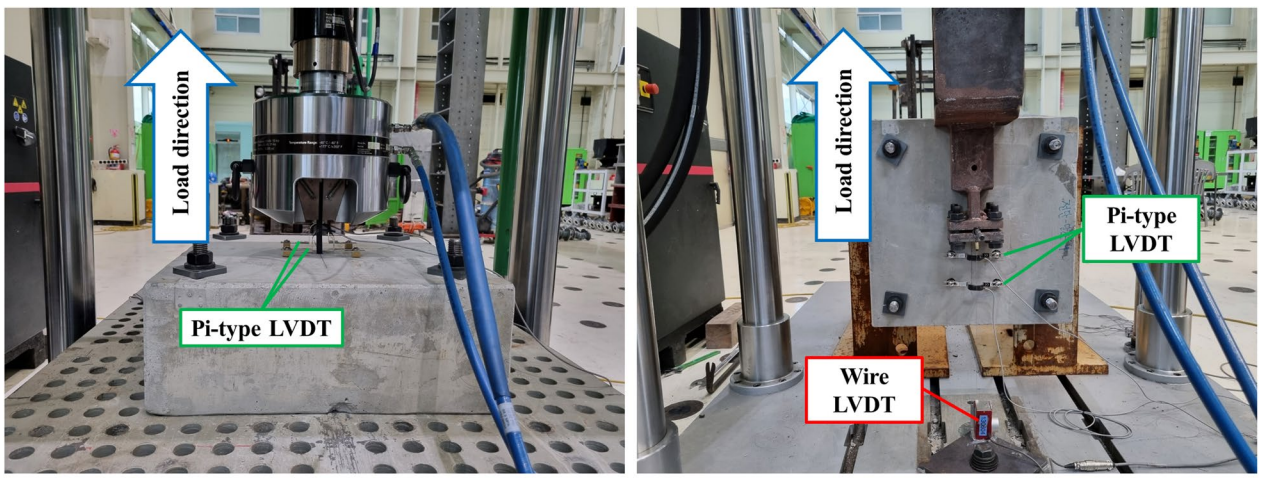

(a) Tension test (b) Shear test

Fig. 7 Test setup

The shear specimens were labeled as S-M-1 to S-M-5 according to the order of loading.

3.2 Making Cracked Concrete Specimens

Several methods have been proposed to generate initial cracks on concrete blocks (Eligehausen et al., 2004; Kim et al., 2010; Lee & Jung, 2021; Mahrenholtz & Eligehausen, 2013; Mahrenholtz & Sharma, 2017). In this experiment, a steel plate was used to generate an artificial crack with a width of 0.5 mm that penetrated the anchor (Kim et al., 2010; Lee & Jung, 2021). Fig. 8 shows the entire process of concrete block fabrication, which is summarized as follows: (a) create a form, (b) fix the insert to the form, (c) install a steel plate 300 mm long by 0.5 mm wide, (d) pour concrete, (e) allow the concrete to initially set, (f) remove the embedded steel plate, (g) remove the form along with the fixing screw that connected the insert to the form, and (h) complete fabrication.

A total of six concrete cylinders were made along with a concrete block cast (KATS, 2019), and they were cured under the same conditions as the blocks. On the first (28 days) and last dates (35 days) of the tension and shear test, compressive tests were performed for three cylinders, according to KS F 2405 (KATS, 2017), and the resulting compressive strengths were 24.98 MPa and 26.48 MPa, respectively. The average of 25.73 MPa was used as the $f_c^{'}$ value when predicting the strength of the specimens.

3.3 Strength Prediction According to ACI 318

The nominal tension and shear strengths (N_n and V_n) of the test specimens were calculated using the design equation of ACI 318. Since the main part of the anchor was installed before the concrete casting, the nominal strengths were determined by assuming that the anchor was a cast-in headed anchor. ACI 318 considers all possible failure modes for tensile and shear loadings, and the weakest failure strength is defined as the tension and shear strength of the anchor. The failure modes of the cast-in anchor for the tensile loading were steel failure, concrete breakout, pullout, and side-face blowout. Steel failure, concrete breakout, and concrete pryout were failure modes for the shear loading. Tables 2 and 3 present the design equation and the corresponding nominal strengths of the specimens for each failure mode of ACI 318.

For both tension and shear strengths, two distinct cases were considered for the nominal strengths relevant to anchor steel failure. The first nominal strengths ($N_{sa,1}$ and $V_{sa,1}$) were related to the high-strength threaded rod used in this experiment, and the standard limit of 860 MPa was specified as the tensile strength of the anchor steel (f_{uta}). The second nominal strengths ($N_{sa,2}$ and $V_{sa,2}$) were relevant to the normal-strength threaded rod for actual future use in the new insert anchor, and $f_{uta}=400$ MPa was applied. The predicted failure modes for tension and shear specimens were concrete breakout and concrete pryout, respectively, and their strengths were the same at 17.93 kN.

4 Results and Discussion

4.1 Tension Tests

After tension testing, the specimens were examined, and the results are shown in Fig. 9. Concrete breakout failure occurred in all five specimens. The initial crack, which was 0.5 mm wide, expanded to approximately 1.0 mm during the monotonic tension loading. No damage was found in any part of the anchor, including the threaded rod and internal thread of the insert, until the experiment

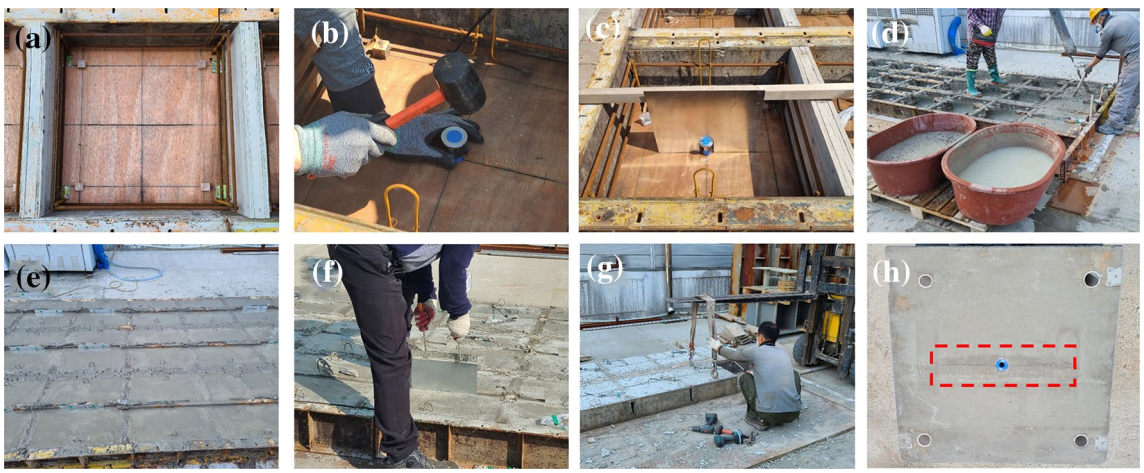

Fig. 8 Fabrication process of cracked concrete blocks

Table 2 Nominal strengths in tension

Failure mode	Design equation	Calculated strength (kN)
Anchor steel failure 1 (high-strength threaded rod)	$N_{sa,1} = A_{se,N} \times f_{uta,h}$	72.50
Anchor steel failure 2 (normal-strength threaded rod)	$N_{sa,2} = A_{se,N} \times f_{uta,n}$	33.72
Concrete breakout failure	$N_{cb} = (A_{Nc}/A_{Nco}) \times \psi_{ed,N} \times \psi_{c,N} \times \psi_{cp,N} \times N_b$	17.93
Pullout failure	$N_{pn} = \psi_{c,P} \times N_p$	239.69
Concrete side-face blowout failure	$N_{sb} = 13 \times c_{a1} \times \sqrt{A_{brg}} \times \lambda_a \times \sqrt{f'_c}$	149.22

N_{sa} nominal steel strength of a single anchor in tension, $A_{se,N}$ effective cross-sectional area of an anchor in tension, N_{cb} nominal concrete breakout strength of a single anchor in tension, A_{Nco} projected concrete failure area of a single anchor if not limited by edge distance or spacing, $\psi_{ed,N}$ breakout edge effect factor used to modify tensile strength, $\psi_{c,N}$ breakout cracking factor used to modify tensile strength, $\psi_{cp,N}$ breakout splitting factor used to modify tensile strength, N_b basic concrete breakout strength of a single anchor in tension in cracked concrete, N_{pn} nominal pullout strength of single anchor in tension, $\psi_{c,P}$ pullout cracking factor, N_p basic single pullout strength, N_{sb} side-face blowout strength of a single anchor in tension, c_{a1} distance from the center of an anchor shaft to the edge of concrete in one direction, A_{brg} net bearing area of the head of insert, and λ_a modification factor to reflect the reduced mechanical properties of lightweight concrete

Table 3 Nominal strengths in shear

Failure mode	Design equation	Calculated strength (kN)
Anchor steel failure 1 (high-strength threaded rod)	$V_{sa,1} = 0.6 \times A_{se,V} \times f_{uta,h}$	43.50
Anchor steel failure 2 (normal-strength threaded rod)	$V_{sa,2} = 0.6 \times A_{se,V} \times f_{uta,n}$	20.23
Concrete breakout failure	$V_{cb} = (A_{Vc}/A_{Vco}) \times \psi_{ed,V} \times \psi_{c,V} \times \psi_{h,V} \times V_b$	51.28
Concrete pryout failure	$V_{cp} = k_{cp} \times N_{cb}$	17.93

V_{sa} nominal steel strength of a single anchor in shear, $A_{se,V}$ effective cross-sectional area of an anchor in shear, V_{cb} nominal concrete breakout strength of a single anchor in shear, A_{Vc} projected concrete failure area of a single anchor for calculation of strength in shear, A_{Vco} projected concrete failure area of a single anchor for calculation of strength in shear if not limited by corner influences, spacing or member thickness, $\psi_{ed,V}$ breakout edge effect factor used to modify shear strength, $\psi_{c,V}$ breakout cracking factor used to modify shear strength, $\psi_{h,V}$ breakout thickness factor used to modify shear strength, V_b basic concrete breakout strength of a single anchor in shear in cracked concrete, V_{cp} nominal concrete pryout strength of a single anchor, and k_{cp} coefficient for pryout strength

was completed. Fig. 10 presents the load–displacement curves of the five tension specimens, and the key results are summarized in Table 4. The maximum tension strength (N_{max}) obtained from the experiment was within the range of 19.75–24.43 kN. The mean tension strength (N_m) was 22.68 kN, which was 26.5% higher than the N_n value (17.93 kN) determined by the ACI 318 design equation (see Table 2). The average displacement where N_{max} was reached [$\delta(N_{max})$] was 0.79 mm.

The coefficient of variation (v) was used to assess the scatter of repeated experimental results. It was determined by dividing the standard deviation by the mean. ACI 355.2 limits the v for the ultimate tension load to within 15%; in this experiment it was 6.88%, i.e., less than half the limit. The v for $\delta(N_{max})$ was determined to be 9.90%. Further, ACI 318 permits the use of experimentally measured strength values in the design, but for this purpose, a 5% fractile with 90% confidence must be used to evaluate the test. The equation for determining the

(a) Concrete block (b) Cast-in insert (c) Threaded rod

Fig. 9 Failure modes observed after monotonic tension tests

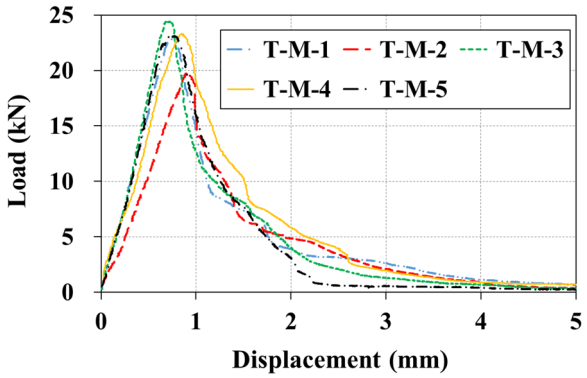

Fig. 10 Load–displacement curves of tension specimens

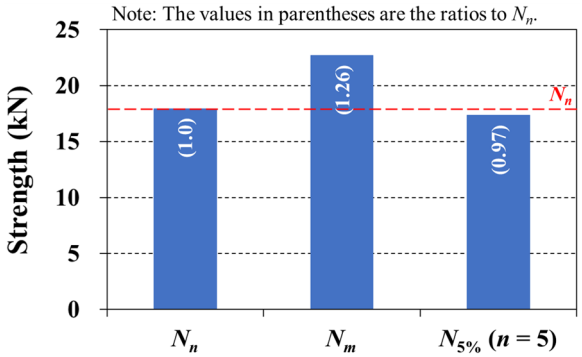

Fig. 11 Comparison of tension strengths

Table 4 Summary of tension test results

Specimen	Failure mode	N_{max} (kN)	$\delta(N_{max})$ (mm)
T-M-1	Concrete breakout	22.84	0.75
T-M-2	Concrete breakout	19.75	0.91
T-M-3	Concrete breakout	24.43	0.69
T-M-4	Concrete breakout	23.30	0.85
T-M-5	Concrete breakout	23.10	0.77
Mean	–	22.68	0.79

characteristic capacity in a test series ($F_{5\%}$) according to ACI 355.2 is given by Eq. (2):

$$F_{5\%} = F_m \times (1 - \mathrm{K}v), \tag{2}$$

where F_m is the mean capacity obtained from the tests, and K is a statistical constant, set to 3.400 in this experiment with five tests (n).

The 5% fractile of N_{max} ($N_{5\%}$) for this experiment calculated by the above equation was 17.37 kN, which was 3.1% smaller than N_n. This was attributed to the application of a relatively large K value, as n in this experiment was not large; when n is assumed to be ∞ (here, K=1.645), $N_{5\%}$ is 20.11 kN, which is 12.2% greater than N_n. Fig. 11 compares the predicted N_n and the anchor's experimental tension strengths (N_m and $N_{5\%}$). N_n differed only negligibly from $N_{5\%}$, and even the strength reduction factor (ϕ) is applied in the actual design. Based on this fact, the ACI 318 design equation for the cast-in headed anchor was determined to be applicable to the prediction of the tension strength of the new insert anchor.

The CCD method assumes that the breakout failure surface angle (α) is approximately 35° for all anchor types, as shown in Fig. 12a, and ACI 318 consequently recommends that the critical edge distance (c_{cr}) be $1.5h_{ef}$. However, anchors with significant d_h values, such as the insert anchor used in this study, have been previously reported to have small failure cone angles and large failure cone projected areas (Karmokar et al., 2021; Lee et al., 2007; Nilforoush et al., 2017, 2018). The c_{cr} and α measured in this experiment are listed in Table 5. The average α for each specimen was approximately 20°, which was smaller than the failure angle of 35° predicted by the CCD method. Accordingly, c_{cr} was observed to be greater than 75 mm ($1.5h_{ef}$). Based on these results, a more stringent condition than that in ACI 318 should be applied for anchor group effects. Therefore, before accumulating more experimental data, the application of $c_{cr} = 2h_{ef}$ (A_{Nc}=$16h_{ef}^2$), which is larger than the current standard of $1.5h_{ef}$ (A_{Nc}=$9h_{ef}^2$), is proposed for the new insert anchor design.

4.2 Shear Tests

The specimens after shear testing are depicted in Fig. 13. The typical concrete pryout failure occurred in all five specimens. During monotonic shear loading, the initial 0.5-mm crack was expanded up to approximately 2.5 mm. Although no specific damage was detected on the insert after the experiment, a significant residual deformation was observed on the threaded rod due to the load in the shear direction, as shown in Fig. 13d. Fig. 14 illustrates the load–displacement curves of the five shear specimens, and the key results are summarized in Table 6. The maximum shear strength (V_{max}) obtained from the experiment ranged from 33.07 to 47.63 kN, with a mean (V_m) of 40.42 kN. This value is noteworthy, as it was 125% greater than the V_n=17.93 kN obtained using the ACI 318 design equation (see Table 3). The average displacement where V_{max} was reached [$\delta(V_{max})$] was 9.93 mm.

The v of V_{max} and $\delta(V_{max})$ was 11.58% and 16.72%, respectively, and the data scatter was greater than that from tension testing. As with the tension test, the 5% fractile of V_{max} ($V_{5\%}$) was calculated using n and v. The resulting value was 24.51 kN, which was 37.0% greater than V_n. Fig. 15 compares the predicted V_n

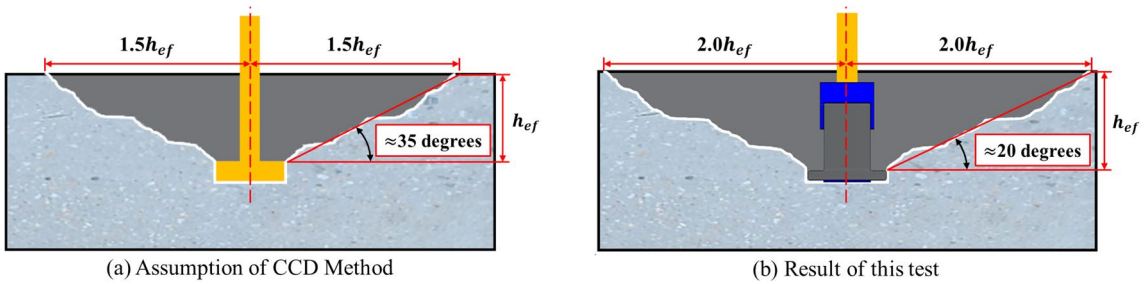

(a) Assumption of CCD Method (b) Result of this test

Fig. 12 Section through failure cone

Table 5 Critical edge distance (c_{cr}) and breakout failure surface angle (α) measured in tension tests

Specimen	Critical edge distance (mm)		Breakout failure surface angle (degree)		
	Max	Min	Max	Min	Mean
T-M-1	188	93	28.17	14.90	21.54
T-M-2	163	91	28.90	17.06	22.98
T-M-3	151	88	29.52	18.33	23.93
T-M-4	215	111	24.16	13.09	18.62
T-M-5	187	81	31.53	14.95	23.24

and experimental shear strengths (V_m and $V_{5\%}$) of the anchor. V_n was determined by concrete pryout failure (Table 3), and the failure mode prediction of the anchor according to ACI 318 was accurate. Furthermore, the ACI 318 design equation for the cast-in headed anchor predicted a strength lower than the experimental value, indicating its suitability for the prediction of the shear strength of the new insert anchor. However, the concrete pryout strength according to the standard equation significantly underestimates the actual insert anchor strength. To facilitate more cost-effective designs, additional research is required to develop an appropriate strength prediction equation.

5 Conclusions

In this study, we investigated the capacity and behavioral characteristics of a new headed cast-in specialty insert anchor. To achieve this objective, three cyclic tension tests were initially performed for the specialty insert with a threaded rod according to AC 446. All experimental specimens reached the target strength without any damage. Next, monotonic tension and shear tests were conducted five times each for the insert anchor in cracked concrete. The following results were obtained:

1. All five specimens under tensile loading failed due to concrete breakout as predicted. There was no damage to any of the anchor parts until the end of the experiment, including the threaded rod and internal thread of the insert. The average N_{max} of the experimentally measured values was 22.68 kN, which was 26.5% greater than N_n. Additionally, the 5% fractile of N_{max} ($N_{5\%}$) was 17.37 kN, which was only 3.1% smaller than N_n. Considering the strength reduc-

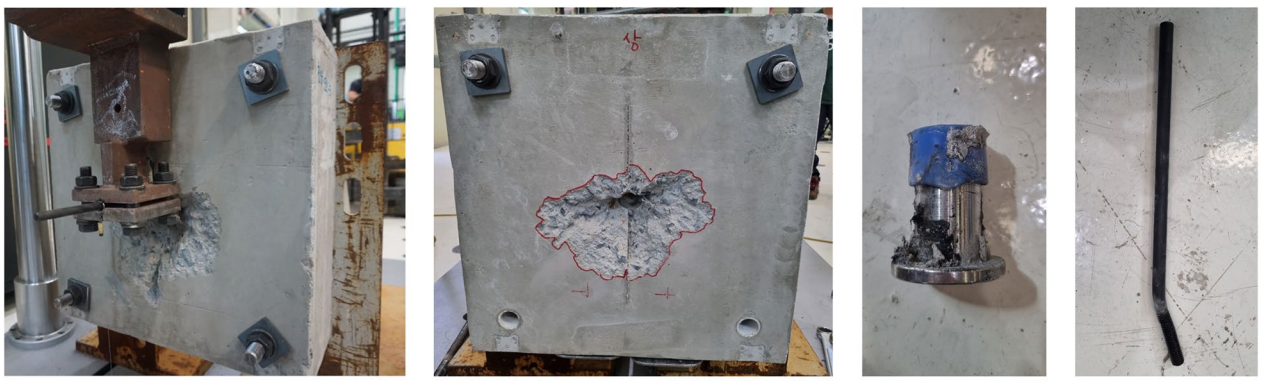

(a) Final failure mode (concrete pryout) (b) Concrete block (c) Cast-in insert (d) Threaded rod

Fig. 13 Failure modes observed after monotonic shear tests

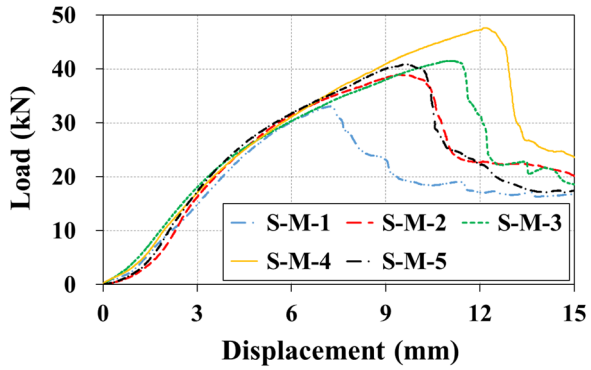

Fig. 14 Load–displacement curves of shear specimens

Table 6 Summary of shear test results

Specimen	Failure mode	V_{max} (kN)	$\delta(V_{max})$ (mm)
S-M-1	Concrete pryout	33.07	7.26
S-M-2	Concrete pryout	38.97	9.50
S-M-3	Concrete pryout	41.51	11.09
S-M-4	Concrete pryout	47.63	12.17
S-M-5	Concrete pryout	40.93	9.64
Mean	–	40.42	9.93

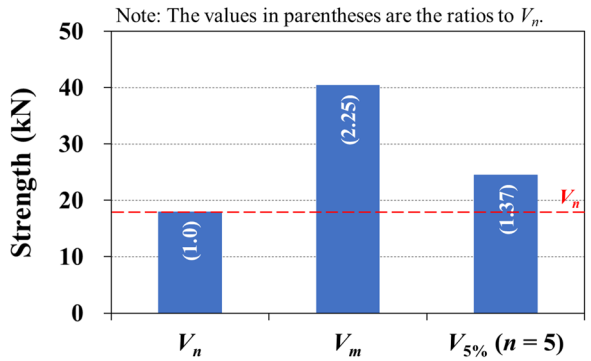

Fig. 15 Comparison of shear strengths

tion applied in the actual design, the ACI 318 design equation for cast-in headed anchors is applicable to predict the tension strength of the new insert anchor.

2. The average breakout failure surface angle (α) of the tension specimens was approximately 20°, which was smaller than the failure angle of 35° predicted by the CCD method. This result is more unfavorable for the anchor group effect, and it was presumed to originate from the insert anchor having a greater d_h than conventional headed anchors. Therefore, a critical edge distance (c_{cr}) of $2h_{ef}$ ($A_{Nc}=16h_{ef}^2$) is proposed, which is greater than the $1.5h_{ef}$ recommended by ACI 318.
3. All five specimens under shear loading failed due to concrete pryout as predicted. The threaded rod showed significant residual deformation due to monotonic shear loading, but no damage was found in any of the parts of the insert until the end of the experiment. The average V_{max} measured during the experiment was 40.42 kN, which was 125% greater than V_n. The 5% fractile of V_{max} ($V_{5\%}$) was 17.37 kN, which was also 37.0% greater than V_n. Based on the experimental results, the ACI 318 design equation may be applicable to predict the shear strength of the new insert anchor, but it significantly underestimates the concrete pryout strength. Therefore, additional research is required to devise a shear strength prediction equation with higher accuracy for a more economic design.

Acknowledgements
This work was supported by project for Collabo R&D between Industry, University, and Research Institute funded by Korea Ministry of SMEs and Startups in 2021 (No. S3103759), and was also supported by the National Research Foundation of Korea (NRF) grant funded by the Korea government (MSIT) (No. 2022R1A2C4001229).

Author contributions
All authors contributed substantially to all aspects of this article. All authors read and approved the final manuscript.

Authors' information
Sang-Deock Jeong, Graduate Student, Division of Architectural and Fire Protection Engineering, Pukyong National University, Busan 48513, Republic of Korea.
Chang-Soo Oh, CEO, Yangsoo Metals Co., Ltd., Ulsan 44993, Republic of Korea.
Chang-Hwan Lee, Associate Professor, Department of Architectural Engineering, Pukyong National University, Busan 48513, Republic of Korea.

Availability of data and materials
The data sets used and analyzed during the current study are available from the corresponding author upon reasonable request.

Declarations

Competing interests
The authors declare that they have no competing interests.

Received: 30 January 2023 Accepted: 16 April 2023
Published online: 17 July 2023

References

ACI (American Concrete Institute). (2019). *Building code requirements for structural concrete (ACI 318M-19) and commentary (ACI 318RM-19)*. Farmington Hills: ACI.
ACI Committee 355. (2019). *Qualification of post-installed mechanical anchors in concrete (ACI 355.2-19) and commentary*. Farmington Hills: ACI.
Delhomme, F., Roure, T., Arrieta, B., & Limam, A. (2015). Static and cyclic pullout behavior of cast-in-place headed and bonded anchors with large embedment depths in cracked concrete. *Nuclear Engineering and Design, 287*, 139–150.

Di Nunzio, G., & Muciaccia, G. (2000). A literature review of the head-size effect on the capacity of cast-in anchors. In *Proceedings of 10th International Conference on Fracture Mechanics of Concrete and Concrete Structures, Bayonne, France*. https://doi.org/10.21012/FC10.239783
Eligehausen, R., Mattis, L., Wollmershauser, R., & Hoehler, M. S. (2004). Testing anchors in cracked concrete. *Concrete International, 26*(7), 66–71.
Filiatrault, A., Perrone, D., Merino, R. J., & Calvi, G. M. (2021). Performance-based seismic design of nonstructural building elements. *Journal of Earthquake Engineering, 25*(2), 237–269.
Fuchs, W., Eligehausen, R., & Breen, J. E. (1995). Concrete capacity design (CCD) approach for fastening to concrete. *Structural Journal, 92*(1), 73–94.
Hoehler, M. S., Mahrenholtz, P., & Eligehausen, R. (2011). Behavior of anchors in concrete at seismic-relevant loading rates. *ACI Structural Journal, 108*(2), 238–247.
ICC-ES (The International Code Council Evaluation Service). (2018). *Acceptance criteria for headed cast-in specialty inserts in concrete* (AC 446). ICC-ES.
Jang, J. B., & Suh, Y. P. (2006). The experimental investigation of a crack's influence on the concrete breakout strength of a cast-in-place anchor. *Nuclear Engineering and Design, 236*(9), 948–953.
Jeon, J. S., Kim, J. H., Oh, C. S., & Lee, C. H. (2021). Tensile and shear strengths of new type of cast-in-place concrete insert anchors under monotonic loading. *Journal of Korean Association for Spatial Structures, 21*(2), 49–56.
Karmokar, T., Mohyeddin, A., Lee, J., & Paraskeva, T. (2021). Concrete cone failure of single cast-in anchors under tensile loading–A literature review. *Engineering Structures, 243*, 112615.
KATS (Korean Agency for Technology and Standards). (2017). *KS F 2405: Standard test method for compressive strength of concrete*. Seoul (Korea): Korean Standards Association.
KATS (Korean Agency for Technology and Standards). (2019). *KS F 2403: Standard test method for making and curing concrete specimens*. Seoul (Korea): Korean Standards Association.
Kazantzi, A. K., Vamvatsikos, D., & Miranda, E. (2020). Evaluation of seismic acceleration demands on building nonstructural elements. *Journal of Structural Engineering, 146*(7), 04020118.
Kim, J. G., Chun, S. C., & An, Y. S. (2022). Pullout tests on M16 stainless post-installed expansion anchor for seismic design in cracked concrete. *Journal of Korea Concrete Institute, 34*(1), 43–50.
Kim, M. K., Choi, I. K., & Kwon, H. O. (2010). Shaking table test for an evaluation of the limit state capacity of an anchor foundation in the case of a seismic event. *Journal of the Earthquake Engineering Society of Korea, 14*(5), 23–31.
Kim, S. Y., Yu, C. S., & Yoon, Y. S. (2004). Sleeve-type expansion anchor behavior in cracked and uncracked concrete. *Nuclear Engineering and Design, 228*(1–3), 273–281.
Lee, N. H., Kim, K. S., Chang, J. B., & Park, K. R. (2007). Tensile-headed anchors with large diameter and deep embedment in concrete. *ACI Structural Journal, 104*(4), 479–486.
Lee, S., & Jung, W. (2021). Evaluation of structural performance of post-installed anchors embedded in cracked concrete in power plant facilities. *Applied Sciences, 11*(8), 3488.
Mahrenholtz, C., Eligehausen, R., & Sharma, A. (2010). Behavior of post-installed concrete undercut anchors subjected to high loading rate and crack cycling frequency. *Proceedings of the 9th U.S. National and 10th Canadian Conference on Earthquake Engineering, Toronto, Canada*, Paper No. 1589
Mahrenholtz, C., & Eligehausen, R. (2013). Dynamic performance of concrete undercut anchors for Nuclear Power Plants. *Nuclear Engineering and Design, 265*, 1091–1100.
Mahrenholtz, C., & Sharma, A. (2017). Testing of anchors and reinforcing bars in concrete under cyclic crack movements. *Journal of Testing and Evaluation, 45*(4), 1326–1337.
Mahrenholtz, P., & Wood, R. L. (2021). Design of post-installed and cast-in-place anchors according to the new EN 1992–4 and ACI 318–19. *Structural Concrete, 22*(2), 650–665.
Merino, R. J., Perrone, D., & Filiatrault, A. (2020). Consistent floor response spectra for performance-based seismic design of nonstructural elements. *Earthquake Engineering & Structural Dynamics, 49*(3), 261–284.
Nilforoush, R., Nilsson, M., & Elfgren, L. (2018). Experimental evaluation of influence of member thickness, anchor-head size, and orthogonal surface reinforcement on the tensile capacity of headed anchors in uncracked concrete. *Journal of Structural Engineering, 144*(4), 04018012.
Nilforoush, R., Nilsson, M., Elfgren, L., Ožbolt, J., Hofmann, J., & Eligehausen, R. (2017). Tensile capacity of anchor bolts in uncracked concrete: Influence of member thickness and anchor's head size. *ACI Structural Journal, 114*(6), 1519–1530.
Ožbolt, J., Eligehausen, R., Periškić, G., & Mayer, U. (2007). 3D FE analysis of anchor bolts with large embedment depths. *Engineering Fracture Mechanics, 74*(1–2), 168–178.
Petersen, D., Lin, Z., & Zhao, J. (2021). Experiments of cast-in anchors under simulated seismic loads. *Engineering Structures, 248*, 113197.
Vita, N., & Sharma, A. (2021). Behaviour of single bonded anchors in non-cracked and cracked steel fiber reinforced concrete under short-time tensile loading. *Engineering Structures, 245*, 112900.
Zamani, N. (2019). *Code provisions for headed cast-in specialty inserts* (p. 41). Washington: STRUCTURE magazine.

Publisher's Note